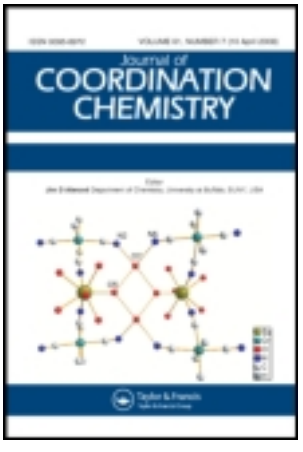

Journal of Coordination Chemistry
Publication details, including instructions for authors and subscription information:
http://www.tandfonline.com/loi/gcoo20

Synthesis and physicochemical properties of fac-[Re(CO)$_3$(κ^2-N,N-dpkfah)Cl], dpkfah=di-2-pyridyl ketone 2-furoic acid hydrazone: the molecular structure of fac-[Re(CO)$_3$(κ^2-N,N-dpkfah)Cl]·acetone

Mohammed Bakir [a] & Colin Gyles [a b]

[a] Department of Chemistry , The University of the West Indies-Mona Campus , Kingston 7, Jamaica, West Indies

[b] Department of Science and Mathematics , University of Technology-Jamaica , 237 Old Hope Road, Kingston 6, Jamaica, West Indies

Published online: 18 May 2011.

To cite this article: Mohammed Bakir & Colin Gyles (2011) Synthesis and physicochemical properties of fac-[Re(CO)$_3$(κ^2-N,N-dpkfah)Cl], dpkfah=di-2-pyridyl ketone 2-furoic acid hydrazone: the molecular structure of fac-[Re(CO)$_3$(κ^2-N,N-dpkfah)Cl]·acetone, Journal of Coordination Chemistry, 64:10, 1743-1757, DOI: 10.1080/00958972.2011.583645

To link to this article: http://dx.doi.org/10.1080/00958972.2011.583645

Journal of Coordination Chemistry
Vol. 64, No. 10, 20 May 2011, 1743–1757

Synthesis and physicochemical properties of *fac*-[Re(CO)$_3$(κ^2-N,N-dpkfah)Cl], dpkfah = di-2-pyridyl ketone 2-furoic acid hydrazone: the molecular structure of *fac*-[Re(CO)$_3$(κ^2-N,N-dpkfah)Cl] · acetone

MOHAMMED BAKIR*† and COLIN GYLES†‡

†Department of Chemistry, The University of the West Indies-Mona Campus, Kingston 7, Jamaica, West Indies
‡Department of Science and Mathematics, University of Technology-Jamaica, 237 Old Hope Road, Kingston 6, Jamaica, West Indies

(*Received 12 January 2011; in final form 24 March 2011*)

Reaction between [Re(CO)$_5$Cl] and di-2-pyridyl ketone 2-furoic acid hydrazone (dpkfah) (**1**) in refluxing toluene gave *fac*-[Re(CO)$_3$(κ^2-N,N-dpkfah)Cl] (**2**). Spectroscopic and electrochemical measurements disclosed sensitivity of **2** to its surroundings. ^{1}H-NMR measurements showed that the amide proton exchanged with solvent protons, and its chemical shift is solvent and temperature dependent, while the chemical shifts of aromatic protons are solvent and temperature independent. Electronic absorption spectra of **2** divulged two intra-ligand charge transfer transitions (ILCT) in protophilic solvents and a single ILCT transition in non-protophilic solvents. Optical measurements on protophilic solutions of **2** established an equilibrium between **2** and its conjugate base, *fac*-[Re(CO)$_3$(κ^2-N,N-dpkfah-H)Cl]$^-$ (**3**). Thermo-optical measurements confirmed that the interconversion between **2** and **3** and gave ΔG^o values of -26.48 and $22.99\,\mathrm{kJ\,mol^{-1}}$, respectively, for the protonation of DMF and DMSO by **2**. Optosensing measurements showed that [MCl$_2$] (M = Zn, Cd, or Hg) in concentrations as low as $1.00 \times 10^{-7}\,\mathrm{mol\,L^{-1}}$ can be detected and determined using protophilic solutions of **2**. Electrochemical measurements showed **2** to be more stable in CH_3CN than DMF. Single-crystal X-ray structural analysis on *fac*-[Re(CO)$_3$(κ^2-N,N-dpkfah)Cl] · acetone (**4**) obtained from an acetone solution of **2** confirmed the solvent–complex interaction and revealed two symmetry-independent molecules in the asymmetric unit. The extended structure of **4** disclosed parallel stacks connected *via* a network of classic and non-classic hydrogen bonds.

Keywords: Synthesis; Rhenium; Di-2-pyridyl ketone 2-furoic acid hydrazone; X-ray crystallography; Electrochemistry; Spectroscopy

1. Introduction

The chemistry of di-2-pyridyl ketone and its oxime and hydrazone derivatives (scheme 1) continues to attract research activities because of their diverse reactivity patterns, physical properties, and applications in catalysis, medicine, environment,

*Corresponding author. Email: mohammed.bakir@uwimona.edu.jm

ISSN 0095-8972 print/ISSN 1029-0389 online
DOI: 10.1080/00958972.2011.583645

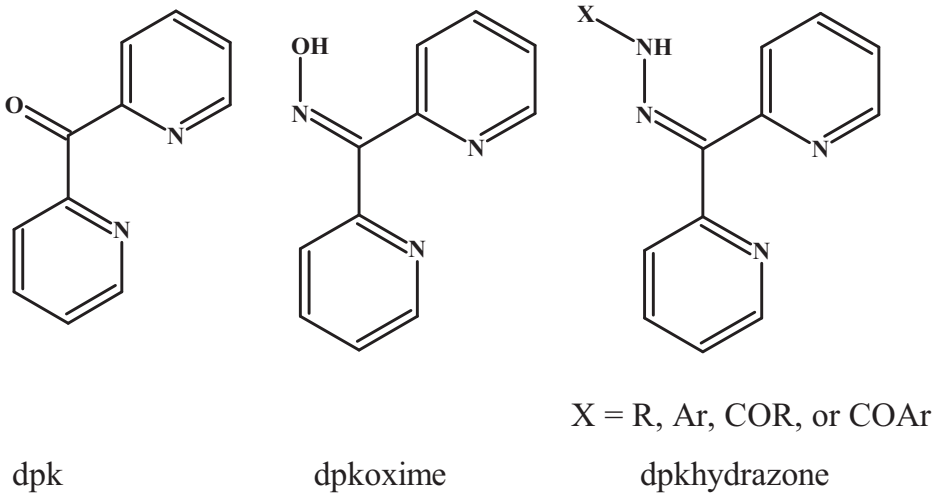

Scheme 1. Di-2-pyridyl ketone and its oxime and hydrazone derivatives.

chemical analysis, etc. [1–31]. Upon coordination to metal, dpk, or its derivatives may utilize all or part of their binding sites to form compounds of different nuclearities. In the monodentate coordination mode, dpk and its derivatives may use a nitrogen of pyridine or the imine backbone. In bidentate coordination mode, dpk or its derivatives may utilize the nitrogens of the pyridine rings or one nitrogen of the pyridine rings and the nitrogen of the imine backbone. In tridentate coordination mode, dpk and its derivatives may utilize a pyridine nitrogen, along with the imine nitrogen and oxygen of an acyl group of a hydrazone backbone. The ligand may also utilize nitrogens of pyridine rings along with an oxygen of the ketone of the hydrazone or semicarbazone backbone. A variety of di-2-pyridyl ketone hydrazones found practical applications as sensitive analytical reagents for the detection and determination of trace amounts of different substrates such as the determination of metal ions in drinking water and pharmaceuticals [11–18]. Biological and therapeutic applications of a variety of di-2-pyridyl ketone hydrazones revealed significant anti-tumor and anti-bacterial activity, and their potential use in chelating therapy for iron overload disease [19–21]. We have been interested in the chemistry of di-2-pyridyl ketone hydrazones and have reported on the synthesis and characterization of a series of compounds such as *fac*-[$M(CO)_3$(κ^2-N,N-L-L)X] (M = Re or Mn; X = Cl or Br and L-L = dpk, dpkoxime, and dpkhydrazone), Mn(κ^3-N,N,O-L-L)$_2$, and [MCl_2(κ^3-N,N,O-L-L)] (M = Zn or Cd and L-L = dpkacylhydrazone) [22–31]. Electrochemical and optical measurements on non-aqueous solutions of *fac*-[$M(CO)_3$(κ^2-N,N-L-L)X], Mn(κ^3-N,N,O-L-L)$_2$, and [MCl_2 (κ^3-N,N,O-L-L)] show sensitivity of these compounds to slight changes in their environment, due to the variety of donor–acceptor sites that allow for potential binding or acid–base inter-conversion between these systems and their surroundings. Although several reports appeared on the use of [dpkfah] as a sensitive analytical reagent for the determination of trace amounts of metal ions in aqueous and non-aqueous media, there has been no report on the coordination chemistry of [dpkfah] (scheme 2) [14–17, 28]. In a previous report we described the structure, electrochemical and optical properties of [dpkfah] and revealed high sensitivity of [dpkfah] to its surroundings [28]. In our efforts

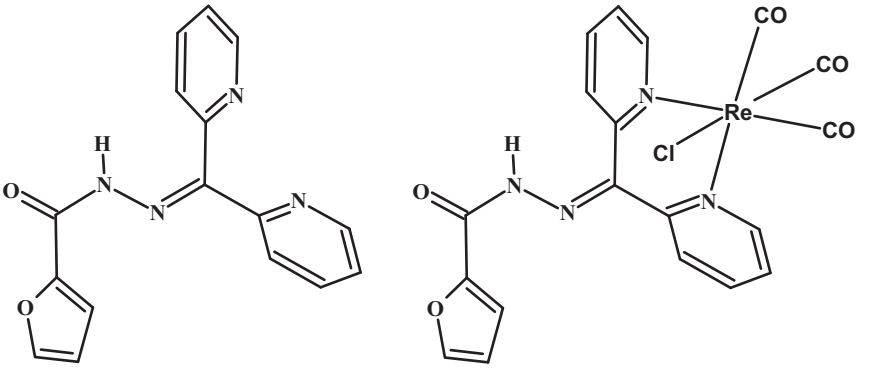

1 2

Scheme 2. [dpkfah] (1) and *fac*-[Re(CO)$_3$ (dpkfah)Cl] (2).

to investigate the chemistry of dpk derivatives, in this report, we describe the synthesis and characterization of the first rhenium compound of [dpkfah], *fac*-[Re(CO)$_3$(κ^2-N, N-dpkfah)Cl] (**2**), and compare the results with those of the uncoordinated [dpkfah] in non-aqueous media.

2. Experimental

2.1. *Reagents and reaction procedures*

[dpkfah] (**1**) was prepared by refluxing a mixture of di-2-pyridyl ketone and 2-furoic acid hydrazide, ethanol, and a few drops of HCl using a standard procedure described previously [28]. All the other reagents were obtained from commercial sources and used without purification.

2.2. *Preparation of fac-[Re(κ^2-N,N-dpkfah)(CO)$_3$Cl] (2)*

A mixture of [Re(CO)$_5$Cl] (200 mg, 0.55 mmol), [dpkfah] (0.19 mg, 0.66 mmol), and toluene (30 mL) was refluxed for 18 h. The resulting reaction mixture was allowed to cool to room temperature and filtered. A yellow solid was filtered off, washed with hexanes and diethyl ether, and dried; yield 200 mg (60%) (Found (%): C, 39.17; H, 2.23; N, 9.18. $C_{19}H_{12}ClN_4O_5Re$ requires (%): C, 38.16; H, 2.02; N, 9.37). Infrared (IR) data (KBr disc, cm^{-1}): ν(C≡O) 2026, 1926, 1886, ν(C=O) 1664 and ν(N–H) 3184 cm^{-1}. ^{1}H NMR (δ ppm): in $CDCl_3$ 9.82 (broad, 0.6 H, NH), 9.42 (d, 1H, dpk), 9.12 (d, 1H, dpk), 8.14 (t, 1H dpk), 8.02 (d, 1H, dpk), 8.00 (t, 1.H dpk), 7.76 (d, 1H, dpk), 7.66 (t, 1H, dpk), 7.56 (broad, 1H, furane), 7.53 (t, 1H, dpk), 7.46 (broad, 1H, furane), and 6.63 (d, 1H, furane); in d_6-acetone 11.26 (broad, 0.8 H, NH), 9.21 (d, 1H, dpk), 9.07 (d, 1H, dpk), 8.32 (t, 1H dpk), 8.29 (d, 1H, dpk), 8.21 (d, 1 H dpk), 8.13 (d, 1H, dpk), 7.79 (overlapped d,t, 2H, 1 H (t) dpk and 1H (d) furane), 7.75 (t, 1H, dpk), 7.41 (broad, 0.9 H, furane), and 6.68 (d, 1H, furane); in d_6-DMSO 12.00 (broad, 0.8 H, NH), 9.05 (d, 1H, dpk), 8.92 (d, 1H, dpk), 8.27 (t, 1H dpk), 8.22 (t, 1H, dpk), 8.03 (d, 1 H dpk),

8.00 (overlapped d, t, 2H, 1 H (t) dpk and 1H (d) furane), 7.75 (t, 1 H, dpk), 7.42 (broad, 0.8 H, furane), and 6.73 (d, 1H, furane). UV-Vis {λ/nm, (ε/cm^{-1} (mol L^{-1})$^{-1}$)}: in CH_2Cl_2 317 (17,200); 275 (18,800); DMSO: 450 (14,198), 322 (15,918); DMF: 450 (30,507), 322 (15,983).

2.3. *Hydrolysis of fac-[Re(κ^2-N,N-dpkfah)(CO)$_3$Cl]*

When a sample of *fac*-[Re(CO)$_3$(κ^2-N,N-dpkfah)Cl] was refluxed in CH_3CN containing a few drops of H_2O *fac*-[Re(CO)$_3$(κ^3-N,O,N-dpkO,OH)] was isolated. The IR and electronic absorption spectra of the isolated *fac*-[Re(CO)$_3$(κ^3-N,O,N-dpkO,OH)] were similar to those reported for *fac*-[Re(CO)$_3$(κ^3-N,O,N-dpkO,OH)] [22].

2.4. *Physical measurements*

Electronic absorption spectra were recorded on a Perkin-Elmer Lambda 19 UV/VIS/NIR spectrometer. Solution ^{1}H NMR spectra were recorded on a Bruker ACE 500 MHz Fourier-transform spectrometer and referenced to the residual protons in the incompletely deuterated solvent. IR spectra were recorded as KBr pellets on a Perkin-Elmer Spectrum 1000 FT-IR Spectrometer. Electrochemical measurements were performed with a Princeton Applied Research (PAR) Model 173 potentiostat/galvanostat and Model 276 interface, in conjunction with a digital Celebris 466 PC. Data were acquired with the EG&G PARC Headstart program and manipulated using Microsoft Excel. Measurements were performed in solutions that were 0.1 mol L^{-1} in N(n-Bu)$_4$PF$_6$. The E_{pa}, E_{pc}, and $E_{1/2} = (E_{pa} + E_{pc})/2$ values were referenced to the saturated calomel electrode (SCE) at room temperature and are uncorrected for junction potentials. Electrochemical cells were of conventional design based on scintillation vials or H-cells. A glassy carbon disc was used as the working electrode and a Pt wire as the counter-electrode.

2.5. *Analytical procedures*

Microanalyses were performed by MEDAC Ltd., Department of Chemistry, Brunel University, Uxbridge, UK.

2.6. *X-ray crystallography*

Brown crystals of *fac*-[Re(CO)$_3$(κ^2-N,N-dpkfah)Cl]·acetone were obtained from an acetone solution of *fac*-[Re(CO)$_3$(κ^2-N,N-dpkfah)Cl] when allowed to stand for several days. A single crystal was selected and mounted on a glass fiber with epoxy cement. A Bruker AXS with Mo-Kα radiation and a graphite monochromator was used for data collection, and the SHELXTL software package version 5.1 was used for structure solution [32, 33]. Cell parameters and other crystallographic information are given in table 1. All non-hydrogen atoms were refined with anisotropic thermal parameters.

Table 1. Crystal data and structure refinement for *fac*-[Re(CO)$_3$(κ^2-N, N-dpkfah)Cl]·acetone.

Empirical formula	$C_{22}H_{18}ClN_4O_6Re$
Formula weight	656.05
Temperature (K)	298(2)
Wavelength (Å)	0.71073
Crystal system	Triclinic
Space group	$P\bar{1}$
Unit cell dimensions (Å, °)	
a	9.0125(12)
b	11.680(2)
c	12.1271(11)
α	80.076(13)
β	76.131(8)
γ	85.168(12)
Volume (Å^3), Z	1219.5(3), 2
Calculated density (Mg m^{-3})	2, 1.787
Absorption coefficient (mm^{-1})	5.136
$F(000)$	636
θ range for data collection	1.75–27.49°
Limiting indices	$-1 \le h \le 11$, $-14 \le k \le 14$, $-15 \le l \le 15$
Reflections collected/unique	6649/6649 [R(int) = 0.0000]
Completeness to $\tau = 27.49$ (%)	99.7
Absorption correction	Empirical
Max. and min. transmission	0.3709 and 0.1704
Refinement method	Full-matrix least-squares on F^2
Data/restraints/parameters	6649/3/595
Goodness-of-fit on F^2	1.047
Final R indices [$I > 2\sigma(I)$]	$R_1 = 0.0478$, $wR_2 = 0.1309$
R indices (all data)	$R_1 = 0.0493$, $wR_2 = 0.1336$
Absolute structure parameter	0.097(19)
Extinction coefficient	0.0064(8)
Largest difference peak and hole	2.949 and −3.896 e Å^{-3}

$R_1 = \sum||F_o| - |F_c||/\sum|F_o|$.
$wR_2 = \{\sum[w(F_o^2 - F_c^2)^2]/\sum w(F_o^2)^2]\}^{1/2}$, where $w = [\sigma^2(F_o^2) + (0.1200P)^2 + 0.00P]^{-1}$ and $P = [\max(F_o^2, 0) + 2F_c^2]/3$.

3. Results and discussion

Following a procedure similar to those described for the synthesis of a variety of rhenium tricarbonyl compounds of the type *fac*-[Re(CO)$_3$(κ^2-N,N-L-L)Cl] where L-L = bidentate α-diimine ligand, the reaction between [Re(CO)$_5$Cl] and dpkfah in refluxing toluene gave *fac*-[Re(CO)$_3$(κ^2-N,N-dpkfah)Cl] (scheme 2) in good yield [22–27]. *Fac*-[Re(CO)$_3$(κ^3-N,O,N-dpkO,OH)] was isolated and characterized from its spectroscopic properties when a sample of *fac*-[Re(CO)$_3$(κ^2-N,N-dpkfah)Cl] was refluxed in CH_3CN that contain few drops of H_2O [22]. The identity of *fac*-[Re(CO)$_3$(κ^2-N,N-dpkfah)Cl] was elucidated from elemental analysis. A number of spectroscopic measurements and X-ray crystallographic analysis of a single crystal of *fac*-[Re(CO)$_3$(κ^2-N,N-dpkfah)Cl]·acetone isolated from an acetone solution of *fac*-[Re(CO)$_3$(κ^2-N,N-dpkfah)Cl] were used as confirmation. A comparison of the IR spectra of *fac*-[Re(CO)$_3$(κ^2-N,N-dpkfah)Cl], *fac*-[Re(CO)$_3$(κ^2-N,N-L-L)Cl], [dpkfah], and other related compounds confirmed the assigned *fac*-geometry and coordination of [dpkfah] [22–28]. The carbonyl ν(C≡O) stretching vibrations appeared at 2026, 1926,

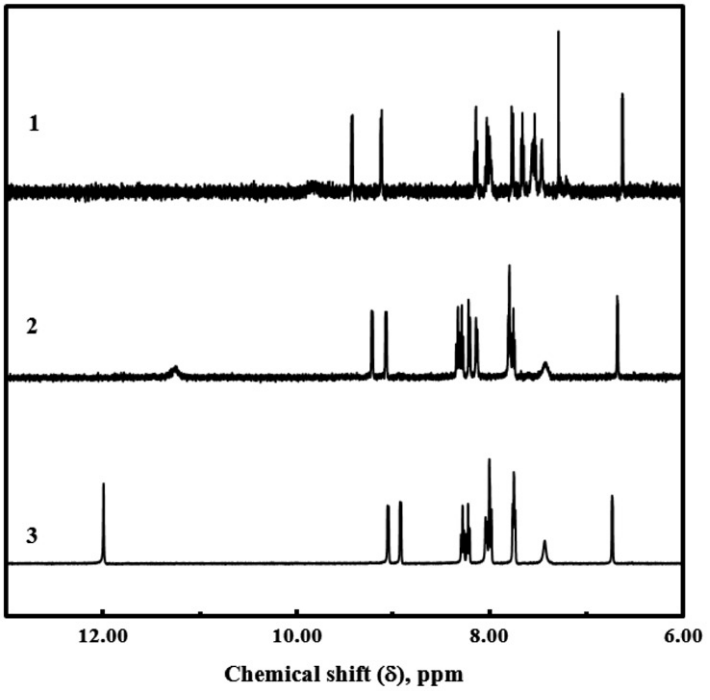

Figure 1. ^{1}H-NMR spectra of *fac*-[Re(CO)$_3$(κ^2-N,N-dpkfahCl] measured in $CDCl_3$, d_6-acetone, and d_6-DMSO.

and 1886 cm^{-1} in the same region reported for a variety of rhenium compounds of the type *fac*-[Re(CO)$_3$(L-L)Cl]. The ν(C=O) stretching vibrations of the hydrazone moiety of *fac*-[Re(CO)$_3$(κ^2-N,N-dpkfah)Cl] and free [dpkfah] appeared at 1664 and 1670 cm^{-1} suggesting no coordination of the carbonyl group of the hydrazone moiety to the metal. The combined ν(C=C) and ν(C=N) vibrations of pyridine of *fac*-[Re(CO)$_3$(κ^2-N, N-dpkfah)Cl] observed between 1606 and 1464 cm^{-1} shift to lower energy compared to the vibrations of free dpkfah observed between 1588 and 1432 cm^{-1} and showed changes consistent with N,N-coordination of [dpkfah].

The ^{1}H-NMR spectra of *fac*-[Re(CO)$_3$(κ^2-N,N-dpkfah)Cl] is solvent dependent (see figure 1 and section 2) pointing to strong solvent–complex interaction. The amide proton appeared at lower frequency in $CDCl_3$ compared to d_6-DMSO and d_6-acetone pointing to weaker hydrogen bonding in $CDCl_3$ compared to d_6-DMSO and d_6-acetone. In protophilic solvents (d_6-DMSO and d_6-acetone) intermolecular hydrogen bonding between the amide proton and the oxygen of the solvent is plausible, while in the case of $CDCl_3$ intra-molecular hydrogen bonding between the amide proton and oxygen of the furane ring to form a five-membered ring is possible. The amide proton exchanged with solvent protons as apparent from the integration of the protons of coordinated dpkfah moiety. The ^{1}H-NMR of *fac*-[Re(CO)$_3$(κ^2-N,N-dpkfah)Cl] is temperature dependent. Variable temperature studies in $CDCl_3$ and d_6-acetone show temperature-dependent amide and residual water protons and temperature-independent aromatic protons. The amide proton and the residual water proton shift to lower

Table 2. Extinction coefficients (±500)[a] and thermodynamic parameters of *fac*-[Re(CO)$_3$(κ^2-N, N-dpkfah)Cl] in DMF and DMSO at 298.15K.

	ε_{446} (mol L^{-1})$^{-1}$cm^{-1}	ε_{322} (mol L^{-1})$^{-1}$cm^{-1}	ΔH^o kJmol^{-1}	ΔS^o JK^{-1}mol^{-1}	ΔG^o kJmol^{-1}	K
DMF	30,507.00	15,983.00	2.30	−96.52	−26.48	4.36×10^4
DMSO	14,198.00	15,918.00	−4.90	−93.55	23.00	9.34×10^{-5}

[a]Calculated using 2.00×10^{-5} mol L^{-1} *fac*-[Re(CO)$_3$(κ^2-N,N-dpkfah)Cl] solution in the presence and absence of 1×10^{-3} mol L^{-1} NaBF$_4$.

frequency upon increasing temperature. A plot of the chemical shift of the amide proton and residual water proton observed at 10.03 and 1.70 ppm and 11.62 and 3.04 ppm in $CDCl_3$ and d_6-acetone, respectively, at 273.15 K gave straight lines with slopes of 574, 282 and 1205, 640 (δ/K) in $CDCl_3$ and d_6-acetone, respectively, pointing to higher sensitivity of the amide and residual water protons of *fac*-[Re(CO)$_3$(κ^2-N,N-dpkfah)Cl] to temperature variation in d_6-acetone compared to $CDCl_3$. This is consistent with the proposed intermolecular hydrogen bonding in d_6-DMSO compared to intra-molecular hydrogen bonding proposed in $CDCl_3$. No evidence of paramagnetic line broadening or unusual shifts of resonances appeared in the spectra of this compound, confirming its diamagnetic character.

The electronic absorption spectra of *fac*-[Re(CO)$_3$(κ^2-N,N-dpkfah)Cl] in different solvents (Supplementary material) confirm the sensitivity of *fac*-[Re(CO)$_3$(κ^2-N, N-dpkfah)Cl] to its surroundings; in DMF and DMSO two electronic transitions appear between 300 and 600 nm and in CH_2Cl_2 a single electronic transition appears (see Supplementary material, section 2, and table 2). The electronic absorption spectra of *fac*-[Re(CO)$_3$(κ^2-N,N-dpkfah)Cl] in DMF in the presence and absence of excess $NaBH_4$ and excess $NaBF_4$ are shown in figure 2. When excess $NaBH_4$ dissolved in DMF was added to a DMF solution of *fac*-[Re(CO)$_3$(κ^2-N,N-dpkfah)Cl] the intensity of the low energy band at 447 nm slightly shifts to 422 nm and its intensity increases, while the intensity of the high energy band at 322 nm in the absence of $NaBH_4$ diminished. The reverse was observed when $NaBF_4$ or KPF_6 was used in place of $NaBH_4$. Similar results were obtained when DMSO was used in place of DMF. These results suggest acid–base interconversion between *fac*-[Re(CO)$_3$(κ^2-N,N-dpkfah)Cl] and its conjugate base *fac*-[Re(CO)$_3$(κ^2-N,N-dpkfah-H)Cl]$^-$ (scheme 3) and allowed for calculation of the extinction coefficients of *fac*-[Re(CO)$_3$(κ^2-N,N-dpkfah)Cl] and *fac*-[Re(CO)$_3$(κ^2-N,N-dpkfah-H)Cl]$^-$ (see table 2 and section 2). The low energy electronic transition is assigned to *fac*-[Re(CO)$_3$(κ^2-N,N-dpkfah-H)Cl]$^-$ and the high energy electronic transition is assigned to *fac*-[Re(CO)$_3$(κ^2-N,N-dpkfah)Cl]. The observed electronic transitions are intra-ligand charge transfer (ILCT) due to π–π* of dpk followed by dpk to furan charge transfer mixed with metal to ligand charge transfer (MLCT). A comparison of the electronic transitions of *fac*-[Re(CO)$_3$(κ^2-N, N-dpkfah)Cl] with those of free dpkfah showed the low-energy electronic transition of *fac*-[Re(CO)$_3$(κ^2-N,N-dpkfah)Cl] shifts to lower energy compared to the free ligand; in the case of CH_2Cl_2 a residual electronic absorption appeared at ~400 nm, corroborating the mixed MLCT and ILCT character of the electronic transitions of *fac*-[Re(CO)$_3$(κ^2-N,N-dpkfah)Cl] [28]. The electronic spectra of dpkfah in CH_2Cl_2 show a single absorption band at 325 nm with an extinction coefficient of

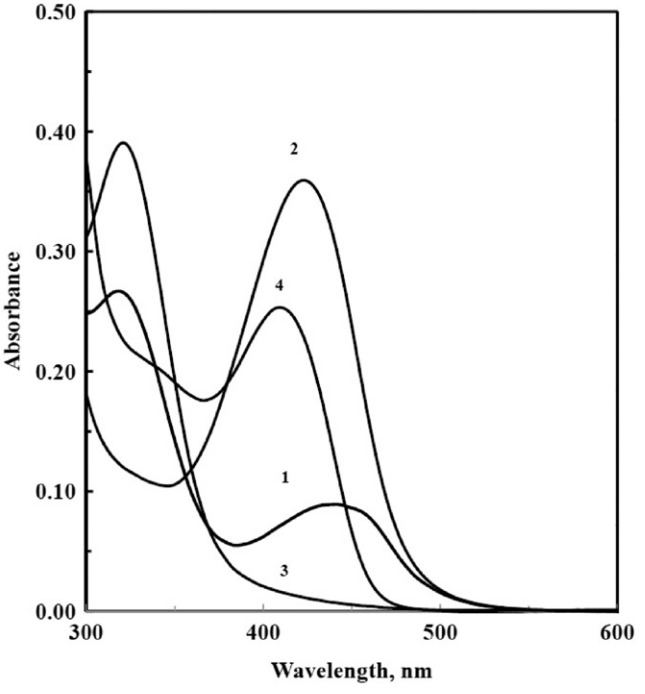

Figure 2. Electronic absorption spectra of 2.00×10^{-5} mol L^{-1} *fac*-[Re(CO)$_3$(κ^2-N,N-dpkfah)Cl] in DMF (1), in the presence of 1.00×10^{-3} $NaBF_4$ (2), in the presence of 1.00×10^{-3} mol L^{-1} $NaBH_4$ (3), and in the presence of 1.00×10^{-3} mol L^{-1} $CdCl_2$ (4).

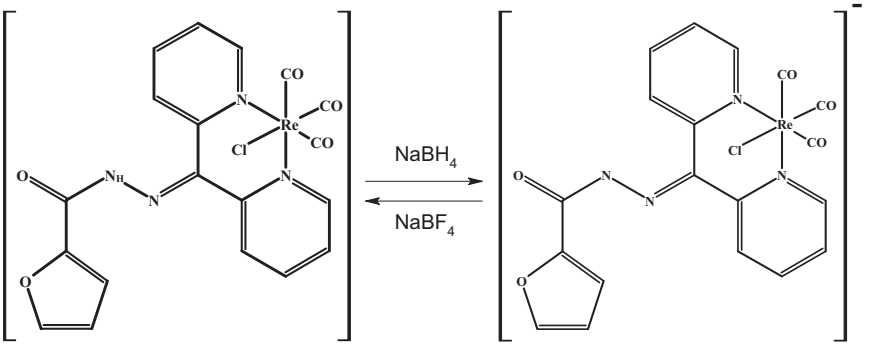

Scheme 3. Acid–base intercoversion between *fac*-[Re(CO)$_3$(κ^2-N,N-dpkfah)CI] and its conjugate base, *fac*-[Re(CO)$_3$(κ^2-N,N-dpkfah-H)CI]$^-$.

$18{,}600 \pm 2000\,(\text{mol L}^{-1})^{-1}$ cm^{-1}, and in DMF two electronic transitions appeared at 396 and 325 nm with extinction coefficients of $21{,}000 \pm 2000$ and $17{,}200 \pm 2000\,(\text{mol L}^{-1})^{-1}$ cm^{-1}, respectively [28].

Electronic transitions of *fac*-[Re(CO)$_3$(κ^2-N,N-dpkfah)Cl] in protophilic solvents are temperature dependent. In DMF as the temperature increases the intensity of the low-

energy electronic transition decreases and the intensity of the high-energy electronic transition increases. The reverse was observed when the temperature decreases or when DMSO was used in place of DMF. These results confirm the reversible interconversion between *fac*-[Re(CO)$_3$(κ^2-N,N-dpkfah)Cl] and *fac*-[Re(CO)$_3$(κ^2-N,N-dpkfah-H)Cl]$^-$ as apparent from the reversible interconversion of their corresponding electronic transitions. The plots of RlnK (Supplementary material) of *fac*-[Re(CO)$_3$(κ^2-N,N-dpkfah)Cl] *versus* $1/T \times 10^3\,\mathrm{K}^{-1}$ in DMF and DMSO gave straight lines that allowed for the calculation of thermodynamic parameters (table 2) for the inter-conversion between *fac*-[Re(CO)$_3$(κ^2-N,N-dpkfah)Cl] and its conjugate base.[†] These results suggest facile interconversion between *fac*-[Re(CO)$_3$(κ^2-N,N-dpkfah)Cl] and *fac*-[Re(CO)$_3$(κ^2-N,N-dpkfah-H)Cl]$^-$ and point to the possible use of *fac*-[Re(CO)$_3$(κ^2-N,N-dpkfah)Cl] in protophilic solvent as a molecular sensor. Free energy changes ($\Delta G^{\varnothing}$) of $+3.5 \pm 0.2$ and $+2.8 \pm 0.2\,\mathrm{kJ\,mol^{-1}}$ were reported for dpkfah in DMSO and DMF, respectively, for the inter-conversion between [dpkfah] and its conjugate base [dpkfah-H]$^-$. These values show that inter-conversion between [dpkfah] and [dpkfah-H]$^-$ is slower than that between *fac*-[Re(CO)$_3$(κ^2-N,N-dpkfah)Cl] and *fac*-[Re(CO)$_3$(κ^2-N,N-dpkfah-H)Cl]$^-$ [28].

When stoichiometric amounts of protophilic solutions of [MCl$_2$] (M = Zn, Cd or Hg) were gradually added to a protophilic solution of *fac*-[Re(CO)$_3$(κ^2-N,N-dpkfah)Cl] a gradual increase in the intensity of the low-energy electronic transition at 440 nm and a gradual decrease in the intensity of the high energy electronic transition at 322 nm were observed. A plot of absorbance of a DMF solution of *fac*-[Re(CO)$_3$(κ^2-N,N-dpkfah)Cl] and *fac*-[Re(CO)$_3$(κ^2-N,N-dpkfah-H)Cl]$^-$ in the presence of [MnCl$_2$] *versus* concentration of [MCl$_2$] is shown in figure 3, indicating that [MCl$_2$] in concentrations as low as $1.00 \times 10^{-7}\,\mathrm{mol\,L^{-1}}$ can be detected using a protophilic solution of *fac*-[Re(CO)$_3$(κ^2-N,N-dpkfah)Cl]. Chemical stimuli (MCl$_2$) in concentrations as low as $1.00 \times 10^{-6}\,\mathrm{mol\,L^{-1}}$ were detected and determined using [dpkfah] in non-aqueous media [28].

The electrochemical properties of *fac*-[Re(CO)$_3$(κ^2-N,N-dpkfah)Cl] in DMF and CH$_3$CN were investigated using voltammetric techniques. Cyclic voltammograms of *fac*-[Re(CO)$_3$(κ^2-N,N-dpkfah)Cl] in DMF and CH$_3$CN are shown in Supplementary material. These voltammograms show strong solvent-dependence consistent with the

[†]For the following inter-conversion:

$$\alpha + \mathrm{S} \leftrightarrows \beta^- + \mathrm{SH}^+ \tag{1}$$

where α = *fac*-[Re(CO)$_3$(κ^2-N,N-dpkfah)Cl] and β^- = *fac*-[Re(CO)$_3$(κ^2-N,N-dpkfah-H)Cl]$^-$, the total absorbance at wavelength λ equals $A_\lambda = \varepsilon_\lambda^\alpha[\alpha] + \varepsilon_\lambda^\beta[\beta] = \varepsilon_\lambda^\beta c + (\varepsilon_\lambda^\alpha - \varepsilon_\lambda^\beta)[\alpha]$, where $c = [\alpha] + [\beta]$ is the total concentration. Thus, $[\alpha] = (A_\lambda - \varepsilon_\lambda^\beta c)/(\varepsilon_\lambda^\alpha - \varepsilon_\lambda^\beta)$ and $[\beta] = (\varepsilon_\lambda^\alpha c - A_\lambda)/(\varepsilon_\lambda^\alpha - \varepsilon_\lambda^\beta)$, so that the equilibrium constant $K = [\beta]^2/[a]$ at temperature T equals

$$K(T) = \frac{(\varepsilon_\lambda^\alpha c - A_\lambda(T))^2}{(A_\lambda(T) - \varepsilon_\lambda^\beta c)(\varepsilon_\lambda^\alpha - \varepsilon_\lambda^\beta)}, \tag{2}$$

(independent of λ and ε's are temperature independent because of the observed isosbestic points). The thermodynamic parameters characterizing the solvent protonation reaction (1) are then obtained according to

$$-\frac{\Delta G^\theta}{T} = R \ln K = \Delta S^\theta - \frac{\Delta H^\theta}{T}. \tag{3}$$

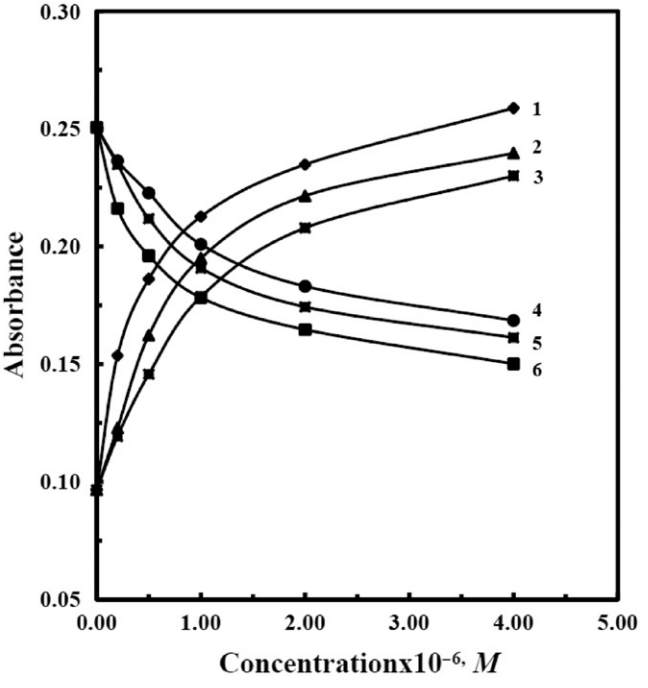

Figure 3. A plot of the absorbance of 2.00×10^{-5} mol L^{-1} *fac*-[$Re(CO)_3(\kappa^2$-N,N-dpkfah)Cl] (4, 5, and 6) and *fac*-[$Re(CO)_3(\kappa^2$-N,N-dpkfah-H)Cl]$^-$ (1, 2, and 3) in DMF (1, 2, and 3) *vs*. concentration of [$ZnCl_2$] (1 and 6), [$CdCl_2$] (2 and 5), [$HgCl_2$] (3 and 4).

spectroscopic measurements in non-aqueous solvents. In DMF upon reductively initiated scan irreversible waves appeared at −1.20, −0.54, +0.92, and +1.16 V, and upon oxidatively initiated scan, waves appeared at +1.36, −0.6, −1.36, and −0.44 V. These voltammograms show electrochemical decomposition of *fac*-[$Re(CO)_3(\kappa^2$-N, N-dpkfah)Cl] in DMF upon oxidation or reduction. This is apparent from the electrochemically generated product waves observed at −0.54, +0.92, and +1.12 V upon oxidation and reductively generated product waves observed at −0.66 and −0.44 V, as well as the +0.16 V shift in the reduction waves observed at +1.20 upon a reductively initiated scan. The electrochemically generated product wave observed at +1.16 V upon reductively initiated scan may be due to $2Cl^-/Cl_2$ oxidation due to the loss of Cl^- upon reduction. The irreversible oxidation at +1.36 upon oxidatively initiated scan and the reduction wave observed at −1.20 V on reductively initiated scan are assigned to $Re^{I\rightarrow II}$ oxidation and $Re^{I\rightarrow 0}$ reduction as they fall in the same region observed for other compounds of the type *fac*-[$Re(CO)_3$(L-L)Cl] [22–25]. In a cyclic scan between −0.5 and −2.5 V irreversible, one-electron reduction appeared at −1.20 V, and a multi-electron reduction appeared at −1.90 V along with electrochemically generated product waves at −2.05, −2.24, and −0.60 V. In a cyclic scan between +0.5 and +2.5 V, an irreversible one-electron oxidation appeared at +1.25 V and a multi-electronic oxidation of at least three electrons appeared at +1.95 V. In CH_3CN, an irreversible reduction appeared at −1.34 V and a quasi-reversible oxidation appeared at $E_{1/2} = +1.55$ V upon oxidatively or reductively initiated scans. In a reductive cyclic scan

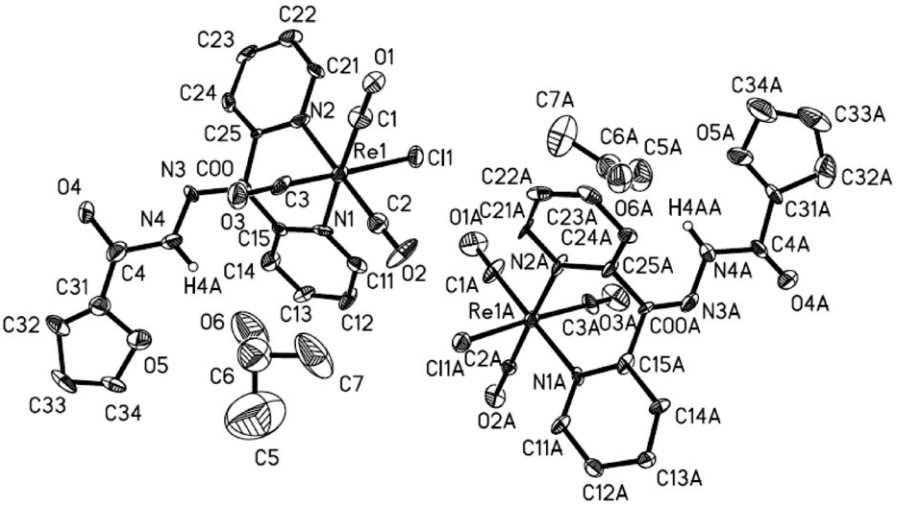

Figure 4. A view of the solid structure of *fac*-[Re(CO)$_3$(κ^2-N,N-dpkfah)Cl] · acetone with thermal ellipsoids drawn at the 30% probability level.

between −0.50 and −2.50 V irreversible, one-electron reduction appeared at −1.30 V and a quasi-reversible two electron reduction appeared at $E_{1/2} = -1.80$ V. In an oxidative scan between +0.50 and +2.50 V, only one-electron quasi-reversible oxidation wave appeared at $E_{1/2} = +1.53$ V. In the voltammograms measured in CH_3CN, no electrochemically generated product waves were observed pointing to the electrochemical stability of *fac*-[Re(CO)$_3$(κ^2-N,N-dpkfah)Cl].

The solid-state structure of *fac*-[Re(CO)$_3$(κ^2-N,N-dpkfah)Cl] · acetone obtained from an acetone solution of *fac*-[Re(CO)$_3$(κ^2-N,N-dpkfah)Cl] when allowed to stand at room temperature for several days was determined using single-crystal X-ray crystallography. A view of the molecular structure of *fac*-[Re(CO)$_3$(κ^2-N,N-dpkfah)Cl] · acetone is shown in figure 4 and selected bond distances and angles are given in table 3. Two molecules appeared in the asymmetric unit and each adopts distorted octahedral geometry with two nitrogens from the pyridine rings of [dpkfah] and two carbons of coordinated carbonyl groups occupying equatorial positions; the axial positions are occupied by a chloride and a coordinated carbonyl group. Variation in bond distances and angles of the molecules in the asymmetric unit may be due to conformational changes during crystallization. This is consistent with spectroscopic and electrochemical measurements that show high sensitivity of *fac*-[Re(CO)$_3$(κ^2-N,N-dpkfah)Cl] to changes in surroundings. The carbonyl groups are facial with average [C–Re–C] angles of 86.9(8)° and 90.8(8)° for each enantiomer in the asymmetric unit. The chelating pyridine rings of dpkfah form six-membered (Re–N–C–C–C–N) metallocycles with pyridine rings in a butterfly formation and N–N bite angles [N–Re–N] of 84.6(6) and 82.2(5)° for the two molecules in the asymmetric unit, similar to those reported for a variety of rhenium compounds containing a six-membered Re–N–C–C–C–N metallocyclic ring, and is larger than those reported for a variety of rhenium compounds of the type *fac*-[Re(CO)$_3$(κ^2-N,N-L-L)Cl] that contain a five-membered Re–N–C–C–N metallocyclic

Table 3. Selected bond lengths (Å) and angles (°) for *fac*-[Re(CO)$_3$(κ^2-N,N-dpkfah)Cl] · acetone.

Re–C(3)	1.81(2)	ReA–C(1A)	1.87(2)
Re–C(1)	1.873(17)	ReA–C(2A)	1.937(18)
Re–C(2)	1.96(2)	ReA–C(3A)	2.007(15)
Re–N(1)	2.161(13)	ReA–N(1A)	2.224(16)
Re–N(2)	2.178(16)	ReA–N(2A)	2.242(15)
Re–Cl	2.469(5)	ReA–ClA	2.484(5)
C(1)–O(1)	1.14(2)	C(1A)–O(1A)	1.21(3)
C(2)–O(2)	1.10(3)	C(2A)–O(2A)	1.14(2)
C(3)–O(3)	1.25(2)	C(3A)–O(3A)	1.04(2)
N(1)–C(11)	1.32(2)	N(1A)–C(11A	1.32(2)
C(15)–C(00)	1.45(2)	C(15A)–C(00A)	1.52(2)
C(00)–N(3)	1.394(19)	C(00A)–N(3A)	1.18(2)
N(3)–N(4)	1.348(18)	N(3A)–N(4A)	1.377(19)
N(4)–C(4)	1.44(3)	N(4A)–C(4A)	1.38(2)
C(4)–O(4)	1.29(2)	C(4A)–O(4A)	1.12(2)
C(31)–O(5)	1.36(3)	C(31A)–O(5A)	1.36(3)
C(6)–O(6)	1.23(4)	C(6A)–O(6A)	1.16(3)
C(6)–C(7)	1.61(5)	C(6A)–C(7A)	1.54(4)
C(3)–Re–C(1)	88.7(9)	C(1A)–ReA–C(3A)	91.7(9)
C(3)–Re–C(2)	85.1(8)	C(2A)–ReA–C(3A)	90.9(7)
C(1)–Re–C(2)	87.0(10)	C(1A)–ReA–C(2A)	89.8(9)
C(1)–Re–N(1)	173.1(8)	C(1A)–ReA–N(1A)	176.0(8)
C(2)–Re–N(1)	96.2(8)	C(2A)–ReA–N(1A)	93.6(6)
C(3)–Re–N(2)	94.8(7)	C(3A)–ReA–N(2A)	91.4(7)
C(2)–Re–N(2)	179.2(9)	C(2A)–ReA–N(2A)	175.2(7)
N(1)–Re–N(2)	84.6(6)	N(1A)–ReA–N(2A)	82.2(5)
C(3)–Re–Cl	178.6(5)	C(3A)–ReA–ClA	173.6(6)
C(1)–Re–Cl	89.9(7)	C(1A)–ReA–ClA	94.0(8)
N(1)–Re–Cl	83.7(3)	N(1A)–ReA–ClA	83.8(4)
O(1)–C(1)–Re	179(2)	O(1A)–C(1A)–ReA	170.4(19)
O(2)–C(2)–Re	175(2)	O(2A)–C(2A)–ReA	176.3(13)
O(3)–C(3)–Re	176.0(15)	O(3A)–C(3A)–ReA	170(2)
C(15)–C(00)–C(25)	124.8(12)	C(15A)–C(00A)–C(25A)	112.0(13)
N(4)–N(3)–C(00)	117.4(14)	C(00A)–N(3A)–N(4A)	118.2(13)
N(3)–N(4)–C(4)	122.8(16)	N(3A)–N(4A)–C(4A)	115.1(14)
O(4)–C(4)–N(4)	115.9(18)	O(4A)–C(4A)–N(4A)	130.5(16)

ring [25–27]. The hydrazone C=N–N–C backbone is coplanar, pointing in the same direction as the axial carbonyl. The amide hydrogen and carbonyl oxygen are *trans*. Bond distances and angles of the coordinated atoms (table 3) are normal and similar to those reported for [dpkfah] and a variety of rhenium compounds of the type *fac*-[Re(CO)$_3$(N–N)X], where N–N = α-diimine ligand and X = anion [25–28].

The extended structure of *fac*-[Re(CO)$_3$(κ^2-N,N-dpkfah)Cl] · acetone shows parallel stacks of *fac*-[Re(CO)$_3$(κ^2-N,N-dpkfah)Cl] · acetone with an extensive network of hydrogen bonding within each stack and the stacks are not connected through any non-covalent interaction (figure 5 and table 4). Non-classical hydrogen bonds Cl $\cdots$ H–C link asymmetric molecules in the unit cell (figure 6a) and each pair of enantiomers is linked to an adjacent pair in the stack through a non-classical hydrogen bond, O $\cdots$ H–C (figure 6b). The solvated acetones are not equivalent; an acetone hydrogen bonds to one *fac*-[Re(CO)$_3$(κ^2-N,N-dpkfah)Cl] through a classic

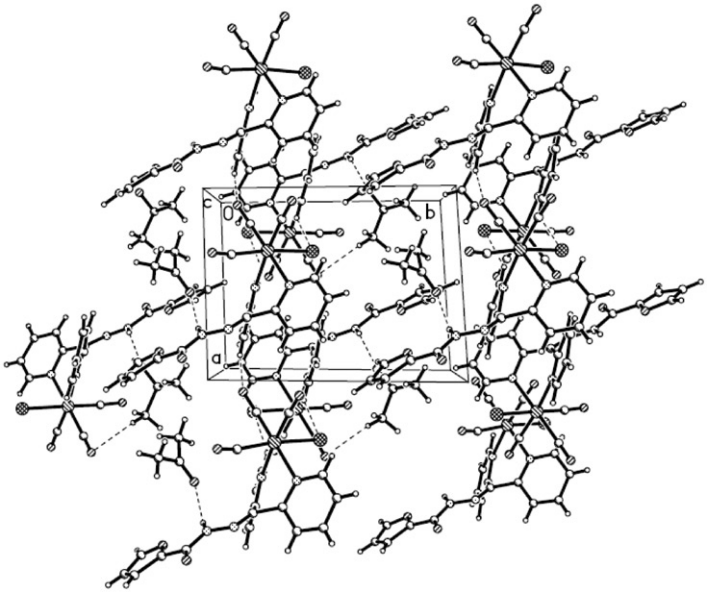

Figure 5. A view of the extended structure of *fac*-[Re(CO)$_3$(κ^2-N,N-dpkfah)Cl] · acetone. Non-covalent bonds are denoted by dashed lines.

Table 4. Hydrogen bond lengths (Å) and angles (°) for *fac*-[Re(CO)$_3$(κ^2-N,N-dpkfah)Cl].

D–H · · · A	d(D–H)	d(H · · · A)	d(D · · · A)	∠(DHA)
N(4)–H(4A) · · · O(6)	0.86	2.53	3.29(4)	147.6
N(4A)–H(4AA) · · · O(6A)	0.86	2.28	3.06(3)	150.2
N(4)–H(4A) · · · O(5)	0.86	2.40	2.75(2)	104.5
N(4)–H(4A) · · · O(6)	0.86	2.53	3.29(4)	147.6
C(6)–H(6A) · · · O(2)	0.96	2.55	3.38(5)	144.2
C(12A)–H(12B) · · · O(4)$^{\#1}$	0.93	2.40	3.13(2)	134.4
C(22)–H(22A) · · · O(4A)$^{\#2}$	0.93	2.56	3.30(2)	136.8
C(24A)–H(24B) · · · O(1A)$^{\#3}$	0.93	2.48	3.32(3)	149.5

Symmetry transformations used to generate equivalent atoms: $^{\#1}x+1, y, z+1$; $^{\#2}x-1, y, z-1$; $^{\#3}x+1, y, z$.

hydrogen bond of the type O · · · H–N while the other acetone binds to *fac*-[Re(CO)$_3$(κ^2-N,N-dpkfah)Cl] through a classic hydrogen bond of the type O · · · H–N between the carbonyl oxygen and amide proton of the hydrazone backbone and a non-classic hydrogen bond of the type O · · · C–H between the oxygen of an equatorial carbonyl with the acetone methyl (figure 6). Bond distances and angles of hydrogen bonds are normal and similar to those reported for a variety of compounds containing such bonds [25–28].

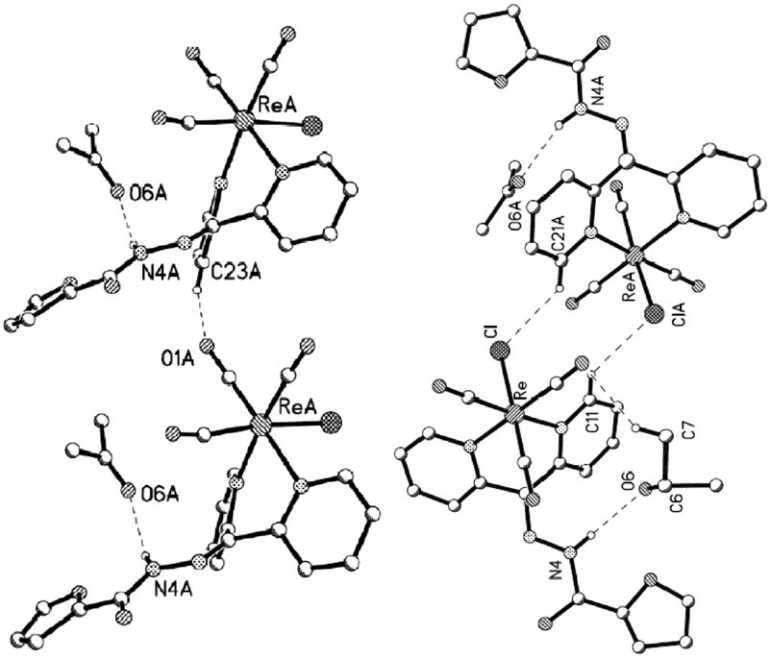

Figure 6. Views of the hydrogen bonds in the extended structure of *fac*-[Re(CO)$_3$(κ^2-N,N-dpkfah)Cl] · acetone.

Due to their diverse coordination, physicochemical properties, and potential applications, work is in progress in our laboratory to further exploit the chemistry of polypyridyl-like ligands and their metal compounds.

4. Conclusion

Fac-[Re(CO)$_3$(κ^2-N,N-dpkfah)Cl] marks the first rhenium compound of dpkfah. Spectroscopic and electrochemical measurements show high sensitivity of *fac*-[Re(CO)$_3$(κ^2-N,N-dpkfah)Cl] to its environment. Facile inter-conversion between *fac*-[Re(CO)$_3$(κ^2-N,N-dpkfah)Cl] and its conjugate base, *fac*-[Re(CO)$_3$(κ^2-N,N-dpkfah-H)Cl]$^-$, was established in protophilic solvents. Electrochemical measurements in DMF show electrochemical decomposition of *fac*-[Re(CO)$_3$(κ^2-N,N-dpkfah)Cl] upon oxidation or reduction, while in CH_3CN the compound is relatively stable. The solid-state structure of *fac*-[Re(CO)$_3$(κ^2-N,N-dpkfah)Cl] · acetone was determined using X-ray crystallography. Two symmetry-independent *fac*-[Re(CO)$_3$(κ^2-N,N-dpkfah)Cl] · acetone are in the asymmetric unit and the extended structure exhibits stacks of chains of *fac*-[Re(CO)$_3$(κ^2-N,N-dpkfah)Cl] · acetone. The chains are locked *via* a network of hydrogen bonds while the stacks are not connected by any non-covalent bonds.

Acknowledgments

We acknowledge Ms Tony Johnson for NMR measurements and the University of the West Indies for funding of this research.

References

[1] C.C. Stoumpos, R. Inglis, O. Roubeau, H. Sartzi, A.A. Kitos, C.J. Milios, C. Aromi, S.P. Perlepes. *Inorg. Chem.*, **49**, 4388 (2010).
[2] N.A. Mangalam, S. Sivakumar, S.R. Sheeja, M.R.P. Kurup, E.R.T. Tiekink. *Inorg. Chim. Acta*, **362**, 4191 (2009).
[3] Z. Chen, F. Liang, S. Zhou, C. Xia, R. Hu. *J. Mol. Struct.*, **827**, 20 (2007).
[4] R. Fandos, C. Hernandez, A. Otero, A. Rodriguez, M.J. Ruiz, P. Terreros. *J. Chem. Soc., Dalton Trans.*, 2990 (2000).
[5] M.A.S. Goher, F.A. Mautner. *Polyhedron*, **18**, 3425 (1999).
[6] G. Alonzo, N. Bertazzi, F. Maggio, F. Benetollo, G. Bombieri. *Polyhedron*, **15**, 4269 (1996).
[7] T.I.A. Gerber, J. Bruwer, G. Bandoli, J. Perils, J.G.H. du Preez. *J. Chem. Soc., Dalton Trans.*, 2189 (1995).
[8] A. Bacchi, L.P. Battaglia, M. Carcelli, C. Pelizzi, G. Pelizzi, C. Solinas, M.A. Zoroddu. *J. Chem. Soc., Dalton Trans.*, 775 (1993).
[9] W.L. Huang, J.R. Lee, S.Y. Shi, C.Y. Tsai. *Transit. Met. Chem.*, **28**, 381 (2003).
[10] S.O. Sommerer, J.D. Baker, W.P. Jensen, A. Hamza, R.A. Jacobson. *Inorg. Chim. Acta*, **210**, 173 (1993).
[11] I. Gaubeur, M.C. da Cunha-Areias, L.H.S. Avila-Terra, M.E.V. Suárez-Iha. *Spectrosc. Lett.*, **35**, 455 (2002).
[12] J.J. Pinto, C. Moreno, M. Garcia-Vargas. *Talanta*, **64**, 562 (2004).
[13] J.G. March, B.M. Simonet, F. Grases. *Analyst*, **124**, 897 (1999).
[14] J.M. Cano Pavon, C. Bosch Ojeda, A. Garcia de Torres, M. Salgado Ordonez. *Anal. Lett.*, **23,**, 1553 (1990).
[15] M. Salgado, C.B. Ojeda, A. Garcia de Torres, J.M.C. Pavon. *Analyst*, **113**, 1283 (1988).
[16] M.S. Ordoñez, A.G. de Torres, J.M.C. Pavon. *Talanta*, **32**, 887 (1985).
[17] A. Garcia de Torres, J.M. Cano Pavón, F. Castafieda. *Mikrochim. Acta [Wien]*, **III**, 375 (1984).
[18] A. Kettrup, T. Seshadri, F. Jakobi. *Anal. Chim. Acta*, **115**, 383 (1980).
[19] S. Kalinowski, D.R. Richardson. *Chem. Res. Toxicol.*, **20**, 715 (2007).
[20] F.R. Pavan, P.I.D.S. Maia, S.R.A. Leite, V.M. Deflon, A.A. Batista, D.N. Sato, S.G. Franzblau, C.Q.F. Leite. *Eur. J. Med. Chem.*, **45,**, 1898 (2010).
[21] A. Dimitrakopoulou, C. Dendrinou-Samara, A.A. Pantazaki, M. Alexiou, E. Nordlander, D.P. Kessissoglou. *J. Inorg. Biochem.*, **102**, 618 (2008).
[22] M. Bakir, J.A.M. McKenzie. *J. Chem. Soc., Dalton Trans.*, 3571 (1997).
[23] M. Bakir, J.A.M. McKenzie. *J. Electroanal. Chem.*, **425**, 61 (1997).
[24] M. Bakir. *J. Electroanal. Chem.*, **466**, 60 (1999).
[25] M. Bakir. *Eur. J. Inorg. Chem.*, 481 (2002).
[26] M. Bakir, O. Brown. *Inorg. Chim. Acta*, **353**, 89 (2003).
[27] M. Bakir, O. Brown. *J. Mol. Struct.*, **930**, 65 (2009).
[28] M. Bakir, C. Gyles. *J. Mol. Struct.*, **649**, 133 (2003).
[29] M. Bakir, O. Green, C. Gyles. *Inorg. Chim. Acta*, **358**, 1835 (2005).
[30] M. Bakir, R.R. Conry, O. Green, W.H. Mulder. *J. Coord. Chem.*, **61**, 3066 (2008).
[31] M. Bakir, R.R. Conry, O. Green. *J. Mol. Struct.*, **921**, 51 (2009).
[32] *Bruker-SHELXTL, Software Version 5.1.*, Bruker AXS, Inc., Madison, Wisconsin, USA (1997).
[33] G.M. Sheldrick. *SHELX97* and *SHELXL97*, University of Göttingen, Germany (1997).